Optical properties of quinolinium ditetracyanoquinodimethanide [Qn(TCNQ)$_2$] and (N-methylphenazinium)$_x$(phenazine)$_{1-x}$(tetracyanoquinodimethanide) [(NMP)$_x$(Phen)$_{1-x}$(TCNQ)]

R. P. McCall
Department of Physics, The Ohio State University, Columbus, Ohio 43210

Ivar Hamberg* and D. B. Tanner
Department of Physics, University of Florida, Gainesville, Florida 32601

Joel S. Miller
Central Research and Development Department, E.I. DuPont de Nemours and Company, Inc., Wilmington, Delaware 19898

A. J. Epstein
Department of Physics and Department of Chemistry, The Ohio State University, Columbus, Ohio 43210
(Received 4 March 1988)

We present here optical-absorption data of quinolinium ditetracyanoquinodimethanide [Qn(TCNQ)$_2$] and (N-methylphenazinium)$_x$(phenazine)$_{1-x}$(tetracyanoquinodimethanide) [(NMP)$_x$(Phen)$_{1-x}$(TCNQ)] for $0.5 \lesssim x \lesssim 0.6$. These materials span the range of electronic structure from commensurate, to commensurate with confined soliton-antisoliton pairs (bipolarons), to incommensurate. The data show that these materials are semiconductors up to 300 K. The semiconducting gap, due mostly to a Peierls distortion, is weakly temperature dependent, decaying slowly as the temperature increases. This behavior, determined by the observation of the totally symmetric a_g vibrational modes of the TCNQ molecule, is similar for all compositions studied and is suggested to be due to the effects of an external cation potential or to Coulomb effects, which vary little with composition. Substantial in-gap absorption is observed and is suggested to be due to the presence of quantum-nucleated and thermally generated bipolarons. The variation of higher-energy electronic transitions with composition corresponds to a crossover from commensurate to incommensurate electronic structure.

I. INTRODUCTION

In this paper we describe the results of a study of the optical properties of quinolinium ditetracyanoquinodimethanide [Qn(TCNQ)$_2$] and (N-methylphenazinium)$_x$(phenazine)$_{1-x}$(tetracyanoquinodimethanide) [(NMP)$_x$(Phen)$_{1-x}$(TCNQ)]. Qn(TCNQ)$_2$ and (NMP)$_x$(Phen)$_{1-x}$(TCNQ) for $x \sim 0.5$ are quasi-one-dimensional charge-transfer salts with quarter-filled conduction bands, i.e., one electron on every two TCNQ sites, and with room-temperature dc conductivities of ~ 100 $\Omega^{-1}\,\mathrm{cm}^{-1}$. For $0.50 \lesssim x \lesssim 0.57$, the (NMP)$_x$(Phen)$_{1-x}$(TCNQ) material is commensurate with confined soliton-antisoliton pairs (bipolarons), while for $x \gtrsim 0.57$ the electronic concentration is incommensurate. Hence these materials provide a unique system to examine the relationship of the electron density and electronic ground state to the optical properties of quasi-one-dimensional materials.

The crystal structure of Qn(TCNQ)$_2$ consists of chains of quinolinium cations and TCNQ molecules along the b axis.[1] The cation chains are disordered due to the random arrangement of the dipoles on the Qn cations. (NMP)$_x$(Phen)$_{1-x}$(TCNQ) is formed from (NMP)(TCNQ) by the substitution of neutral phenazine, Phen, for up to 50% of the NMP's.[2] When $x=0.50$, each NMP contributes one electron to the TCNQ chain while Phen donates no electrons. Thus, (NMP)$_{0.5}$(Phen)$_{0.5}$(TCNQ) is a quarter-filled-band compound. The crystal structure of (NMP)(TCNQ) (Refs. 3 and 4) remains basically unchanged by replacement of up to 50% of the NMP's.[2] For $x=0.5$ the NMP and Phen molecules alternate along the chain and a high degree of order is obtained. For NMP concentration slightly larger than the quarter-filled-band limit, the excess NMP molecules are randomly inserted into the NMP-Phen stacks.[5]

The dc conductivity of Qn(TCNQ)$_2$ (Ref. 6) and (NMP)$_x$(Phen)$_{1-x}$(TCNQ) (Ref. 7) for $x \sim 0.5$ is found to increase slightly upon cooling, reaching a plateau in the range 200–240 K and then decreasing rapidly with further cooling. The details of this behavior change with x.[7,8] Several models have been presented to explain the temperature variation of the conductivity, including (1) disorder-induced localization models,[6,9] (2) a random barrier model,[10] (3) a semiconductor model,[8] and (4) a soliton model.[7,11]

In these materials a large Coulomb repulsion U exists between two electrons that occupy the same site, leading to a splitting of the conduction band, so that those states that correspond to doubly occupied sites are separated from the singly occupied states by a large gap. In this

strongly interacting limit, the lower band is half-filled. Evidence of large-U behavior is found from diffuse x-ray scattering,[10] thermoelectric power,[12,13] and magnetic susceptibility.[7,14]

Peierls[15] has shown that for a one-dimensional metal with no disorder, with a partially filled band (at $T=0$), and with a finite electron-phonon coupling, the regular chain structure is unstable against a static distortion of the lattice and the formation of a charge-density wave (CDW). This distortion causes a splitting at the Fermi level, rendering the material a semiconductor. For the quarter-filled large-U salts, the distortion manifests itself as a commensurate dimerization or pairing of TCNQ molecules so that the unit cell doubles in the chain-axis direction. The lowering of the electronic energy of filled states near the Fermi level is greater than the increase in lattice energy due to the distortion, making the Peierls-distorted state the ground state. For $0.50 \lesssim x \lesssim 0.57$ the distortion is commensurate with excess electrons beyond the $x=0.50$ commensurate value in confined soliton-antisoliton pairs, while for $x \gtrsim 0.57$ the distortion is incommensurate.

Measurements of the optical absorption by $Qn(TCNQ)_2$ and $(NMP)_x(Phen)_{1-x}(TCNQ)$ for $0.50 \lesssim x \lesssim 0.59$, which we present here, support the idea that these compounds are semiconductors at all temperatures on account of a Peierls distortion of the system and the presence of a small external potential for all x. At low temperature the gaps are comparable to those inferred from dc conductivity. The presence of a substantial and temperature-dependent in-gap absorption may be related to quantum-nucleated, doping-generated, and thermally generated bipolarons. Variation with x of the high-energy electronic transitions may reflect the crossover from commensurate to incommensurate electronic structure.

The infrared spectra show the TCNQ a_g vibrational modes, suggesting that a Peierls distortion occurs in these salts. It is well known that these totally symmetric modes, normally infrared inactive, become active for polarization along the chain axis due to phase oscillations.[16] Because of the involvement of the electrons, the oscillator strength associated with these phase phonons is very large. When their frequencies are below the electronic energy gap, they appear as ordinary resonances, whereas when their frequencies overlap the electronic continuum, they have the Fano[17] shape: an antiresonance, or dip, preceeded by a peak on the low-frequency side.

The strength of the Peierls distortion is thought to vary with temperature. This dependence is most easily seen by observing the change with temperature of the oscillator strengths of the a_g vibrational modes.[18–20] Temperature-dependent absorption measurements on powder-KCl samples of (TTF)(TCNQ) (TTF denotes tetrathiofulvalene) indicate a rapid growth of the vibrational features that coincides with the Peierls transition temperature at 53 K.[19] Spectra of powders of $(MEM)(TCNQ)_2$ (MEM denotes methylethylmorpholinium) suspended in mineral oil on CsI windows[20] reveal similar information through a strong increase in the integrated intensity as the temperature is lowered in the range 310–380 K.

Several models have been proposed to explain the temperature variation of the Peierls gap. Conwell and Howard have introduced models that describe the variation in terms of the presence of solitons and bipolarons and the presence of an external potential due to cation chains.[11,21]

The next section of this paper describes sample-preparation and optical techniques used in this study, while the following section contains the absorption data. A detailed discussion in Sec. IV is followed by a summary in the final section.

II. EXPERIMENTAL TECHNIQUES

A. Sample preparation

Samples of $Qn(TCNQ)_2$ and $(NMP)_x(Phen)_{1-x}$-(TCNQ) for $0.50 \lesssim x \lesssim 0.59$ were prepared by the previously described method.[2] The relative NMP composition is accurate to ± 0.015, so that the composition with minimum NMP prepared, i.e., $x=0.49$, is most likely $x=0.50$. The needle-shaped crystals were quite small, ruling out reflection measurements. Therefore, absorption measurements were made on polycrystalline samples prepared by grinding and mixing each sample with an insulating host (KCl or paraffin) and pressing the mixture into a pellet. The typical size of the TCNQ crystals in these samples was several micrometers and the filling fractions were very low. Thus, the crystals were suspended in the host material and the effective absorption coefficients of the TCNQ compounds could be determined after correcting for the absorption and reflection of the host. KCl was used for measurements from 500 to 40 000 cm^{-1}, while paraffin was used from 30 to 700 cm^{-1}.

The composite samples were prepared by placing a specific amount of sample with a specific amount of KCl single crystals or paraffin into a vial and grinding in a liquid-nitrogen-cooled freezer mill. This grinding process produced a powdered sample that had small crystals of the material uniformly dispersed throughout the host material. Because only small amounts of the samples were available, care was taken to remove as much of the powdered sample from the vial as possible. If any material was lost, it was assumed that because both the TCNQ salts and the host material were uniformly mixed, the volume fraction was not affected.

The powdered sample was placed in a $\frac{5}{8}$-in.-diam evacuable die and pressed to form a pellet. For KCl, the powder was pressed to ~ 9 kbar (128 000 psi) and for paraffin, ~ 1 kbar (16 000 psi). This procedure produced pellets that were uniform in color, ranging from light green to dark blue-green. Volume fractions for the KCl-host samples were $\sim 0.1\%$ or less, while the paraffin-host samples were $\sim 0.5\%$.

B. Absorption measurements

The temperature-dependent absorption measurements were made using two types of Michelson interferometers: single-scan and rapid-scan. The home-built single-scan interferometer[22,23] with a 1.2-K bolometer detector was

used in the range 30–700 cm^{-1} to study the paraffin-host samples. Measurements with this instrument were made using standard light-chopping and lock-in–amplifier techniques. The interferometer and lock-in amplifier were interfaced to a DEC LSI-11 minicomputer for data acquisition and analysis. Low-temperature measurements were made by placing the samples in the detector cryostat.

Between 500 and 4000 cm^{-1} a Digilab FTS-14 rapid-scan interferometer was used to study KCl-host samples. Samples were attached to the cold finger of an Air Products Helitran continuous-flow refrigerator for the low-temperature measurements.

Spectra up to 40 000 cm^{-1} were obtained at room temperature using a Perkin-Elmer grating monochromator.[22] Again, standard lock-in detection techniques were used.

C. Data analysis

The transmittance T of the composite sample is given by

$$T=\frac{(1-R)^2e^{-\alpha x}}{1-R^2e^{-2\alpha x}}\ , \tag{1}$$

where x is the thickness of the sample and R the reflectance. The absorption coefficient α is dependent on the absorption of the TCNQ salt, α_{TCNQ}, and that of the insulating host, α_{host}, viz.,

$$\alpha=f\alpha_{TCNQ}+\alpha_{host}\ , \tag{2}$$

where f is the volume filling fraction of the TCNQ salt in the host material. This expression for α is obtained from the theory of Maxwell Garnett,[24] which expresses the average response of an inhomogeneous material in terms of that of the individual constituents. For the mixtures used in this study, the filling fractions of the TCNQ salts were below 0.005, so that only leading terms in f have been considered. The reflectance of the composite samples, as expected because of the low filling fractions, was equal to that of the host. Thus the absorption coefficient of the polycrystalline samples can be calculated from

$$\alpha_{TCNQ}=-\frac{1}{fx}\ln T+\frac{2}{fx}\ln(1-R_{host})-\frac{\alpha_{host}}{f}\ . \tag{3}$$

The transmittance of the composite is the quantity measured with f and x being sample-dependent parameters. Equation (3) assumes that R is small, so that the R^2 term in the denominator of Eq. (2) can be neglected.

The reflectance of the host material, R_{host}, and the absorption coefficient of the host, α_{host}, are dependent on the particular host used. The reflectance of paraffin was determined by measuring the far-infrared absorption of a pure paraffin pellet.[25] This measurement gave a dc value of the transmission, which, in turn, was used to determined the reflectance of paraffin using Eq. (1). (The absorption of an insulator extrapolates to zero at zero frequency.[26]) A value of $R=0.0125$ was found for paraffin at zero frequency and was assumed to be constant over all frequencies in the far infrared. The absorption coefficient, α_{para}, could then be calculated from the transmittance. The reflectance of KCl was determined from the frequency-dependent index of refraction,[27] n, with $R=[(n-1)/(n+1)]^2$. The reflectance is quite constant over the frequency range of interest (500–40 000 cm^{-1}) at about 0.03. Transmission measurements of KCl pellets then gave the absorption coefficient, α_{KCl}.

III. EXPERIMENTAL RESULTS

The infrared-absorption coefficients for $Qn(TCNQ)_2$ and $(NMP)_x(Phen)_{1-x}(TCNQ)$ for $x=0.49$, 0.53, 0.55, 0.56, 0.57, and 0.59 are all similar. Figure 1 shows the far-infrared absorption of $Qn(TCNQ)_2$ at 6 K,[28,29] and typical absorption data for $(NMP)_{0.55}(Phen)_{0.45}(TCNQ)$ at 25 K in the far infrared.[30] Figures 2–4 show the temperature dependence of the absorption data of $Qn(TCNQ)_2$ and $(NMP)_x(Phen)_{1-x}(TCNQ)$ for $x=0.49$, 0.53, 0.55, 0.56, 0.57, and 0.59 over the frequency range 100–3000 cm^{-1}. Figure 5 shows the room-temperature absorption data for $x=0.49$, 0.53, 0.55, and 0.59 in the range 700–40 000 cm^{-1}.[31]

Several important features from the data are evident: (1) the absorption is quite low at 100 cm^{-1}, but increases by a factor of about 30 at 3000 cm^{-1} in all samples shown. Note that there is qualitatively different temperature dependence at low and high frequencies. There is increased absorption for increasing temperature at frequencies below about 700 cm^{-1}, but a reduction in absorption

TABLE I. a_g normal modes of $(NMP)_{0.55}(Phen)_{0.45}(TCNQ)$, $Qn(TCNQ)_2$, and $[TCNQ]^-$.

Vibrational mode	$Qn(TCNQ)_2$ (cm^{-1})	$(NMP)_{0.55}(Phen)_{0.45}(TCNQ)$ (cm^{-1})	$[TCNQ]^-$ [a] (cm^{-1})
ν_1			3052
ν_2	2218	2210	2206
ν_3	1605	1612	1615
ν_4	1425	1420	1391
ν_5	1195	1205	1196
ν_6	950	955	978
ν_7	691	697	725
ν_8	600	600	613
ν_9	306	300	337
ν_{10}	124	117	148

[a]Reference 32.

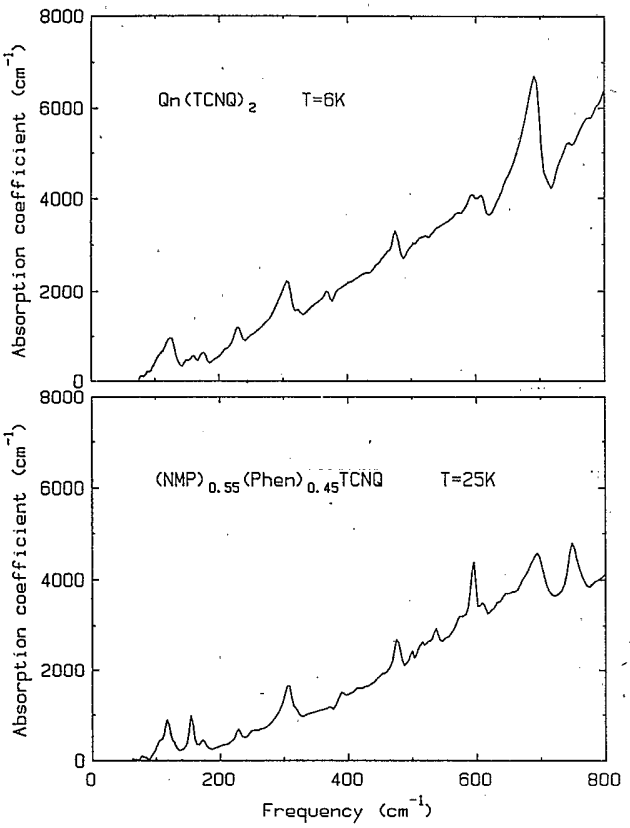

FIG. 1. Far-infrared absorption coefficient of $Qn(TCNQ)_2$ at 6 K (top) and $(NMP)_{0.55}(Phen)_{0.45}(TCNQ)$ at 25 K (bottom).

as the temperature increases at higher frequencies. (2) There are several sharp and broad minima and maxima throughout the infrared region shown that are associated with molecular vibrations in the material. The strongest of these features correspond very closely in position to nine of the ten a_g totally symmetric modes[32] of $[TCNQ]^-$. These modes are listed in Table I for $Qn(TCNQ)_2$ and $(NMP)_{0.55}(Phen)_{0.45}(TCNQ)$ along with

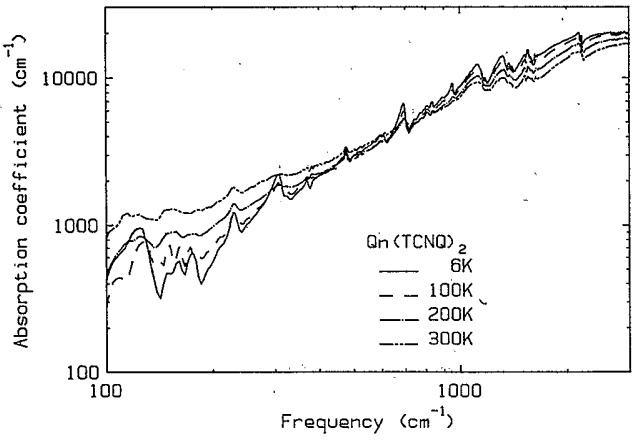

FIG. 2. Absorption coefficient vs frequency for $Qn(TCNQ)_2$ at 6, 100, 200, and 300 K. Note the logarithmic scales.

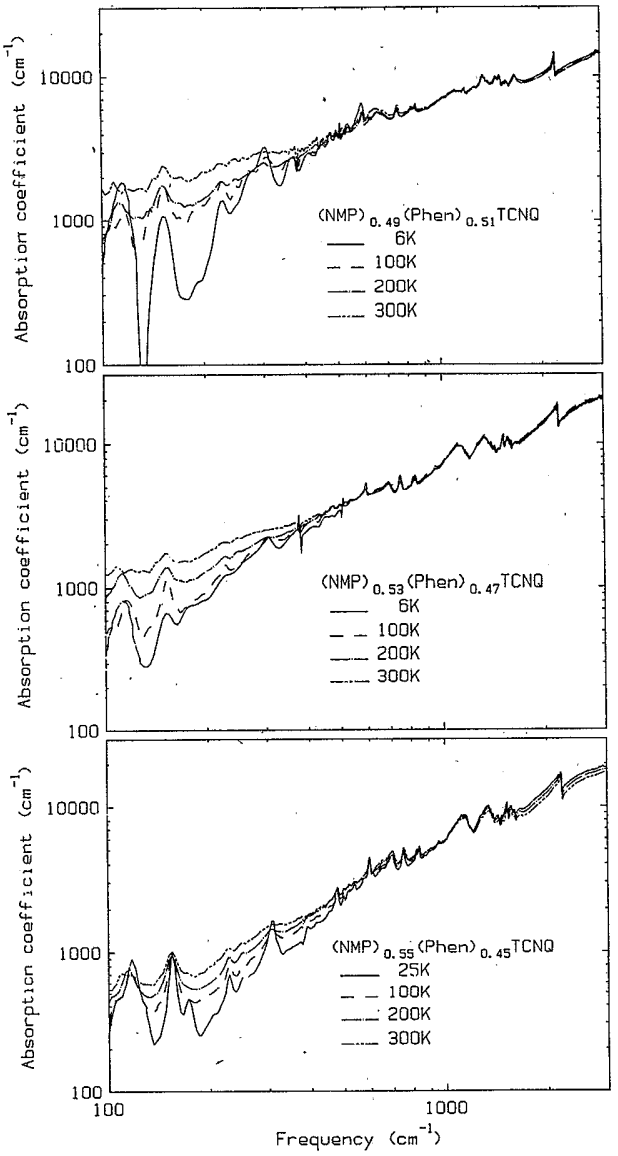

FIG. 3. Absorption coefficient frequency of $(NMP)_x(Phen)_{1-x}(TCNQ)$ for $x=0.49$ (top), 0.53 (middle), and 0.55 (bottom).

those observed for $[TCNQ]^-$ from Bozio *et al.*[32] The a_g modes of all other samples in the NMP-Phen system correspond closely to those listed for the $x=0.55$ sample. (The other vibrational modes are due to other normal modes of the TCNQ molecule or the cations.) The a_g modes have been observed in other TCNQ salts as well, e.g., $(TEA)(TCNQ)_2$ (TEA denotes triethylammonium),[33] $Cs_2(TCNQ)_3$,[22] (TTF)(TCNQ),[19] and $(MEM)(TCNQ)_2$.[34] The temperature dependence of the strengths of the a_g modes is also readily observable, as seen, for example, in the 950-cm^{-1} mode for $Qn(TCNQ)_2$ in Fig. 6. Note that the a_g modes with frequencies below about 950 cm^{-1} are resonances, while those above 950 cm^{-1} are antiresonances. (3) The sample-dependent spectra of $(NMP)_x(Phen)_{1-x}(TCNQ)$ for $x=0.49$, 0.53, 0.55, and 0.59, shown in Fig. 5, exhibit four prominent peaks at

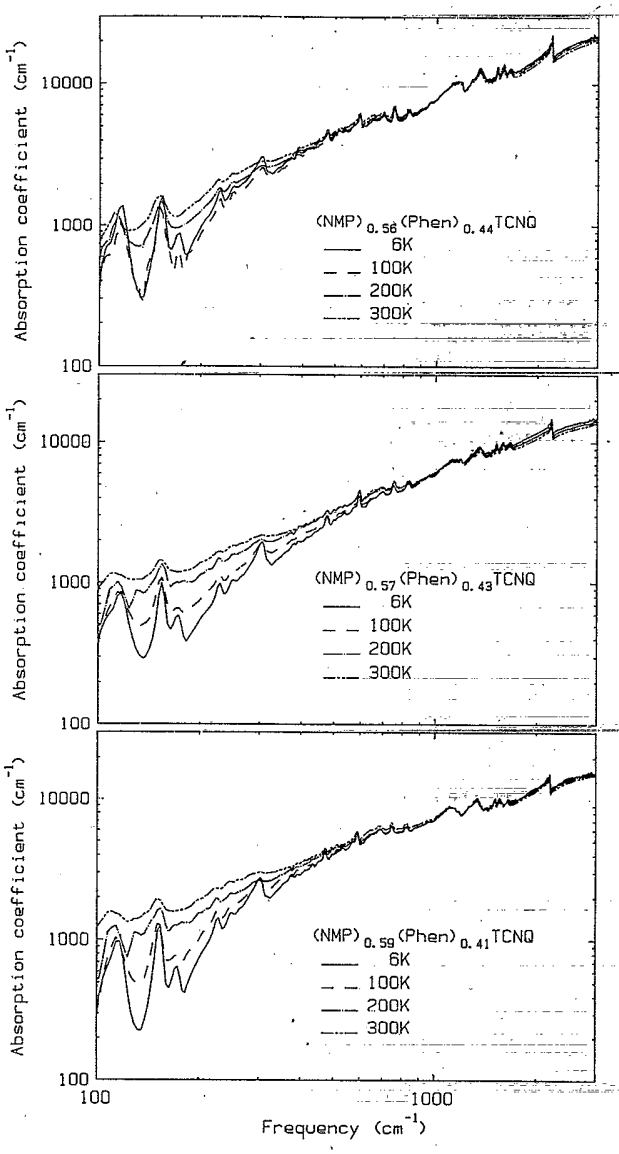

FIG. 4. Absorption coefficient vs frequency of $(NMP)_x(Phen)_{1-x}(TCNQ)$ for $x=0.56$ (top), 0.57 (middle), and 0.59 (bottom).

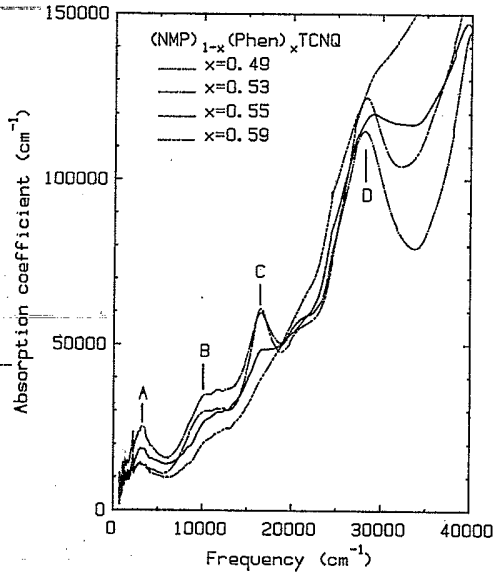

FIG. 5. Absorption coefficient of $(NMP)_x(Phen)_{1-x}(TCNQ)$ for $x=0.49$, 0.53, 0.55, and 0.59 at 300 K.

$A=3500$ cm^{-1} (0.4 eV), $B=10\,000$ cm^{-1} (1.2 eV), $C=16\,000$ cm^{-1} (2.0 eV), and $D=28\,000$ cm^{-1} (3.4 eV). The peaks become less pronounced with increasing x.

IV. DISCUSSION

A broad absorption is observed that begins increasing at ~ 100 cm^{-1} and peaks at 3500 cm^{-1}. This absorption band is ascribed[35] to charge transfer from anion to neutral TCNQ molecules (CT1). The absence of absorption for frequencies below 100 cm^{-1} at low temperatures demonstrates that there is a gap in the density of states at the Fermi level, in contrast to predictions of disorder centered models.

The presence of the a_g vibrational modes in the optical spectra has been shown[16] to be due to the presence of CDW phase oscillations. The CDW's may arise from several possible sources: (1) a periodic distortion of the molecular lattice (the Peierls distortion); (2) Coulomb interactions for which U, the on-site interaction, is large compared to V_1 and V_2, the nearest-neighbor and next-nearest-neighbor interactions;[36,37] or (3) an external potential V_0 arising from the donor-chain structure.[16,21] The coupling of the conduction electrons to the out-of-phase oscillations (the electron-phonon, e-ph, coupling)

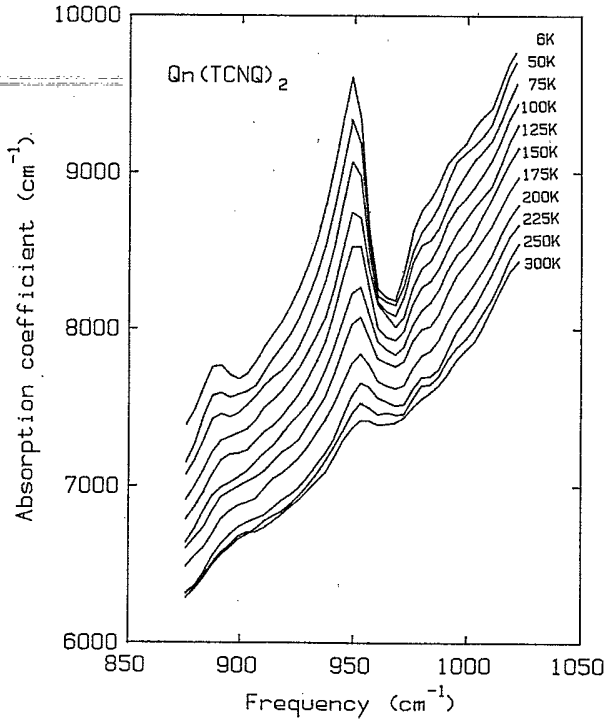

FIG. 6. Temperature dependence of the absorption coefficient of $Qn(TCNQ)_2$ at 950 cm^{-1}.

and to the site nonequivalence of the TCNQ molecules in the chains give rise to nonzero flucutations of the local electronic density (phase oscillations or phase phonons). These fluctuations induce a dipole moment, polarized in the direction of the chain, that causes the normally infrared-inactive a_g modes to become infrared active.

The infrared-absorption spectrum is thus a sum of the contribution due to single electron transitions between the conduction and valence bands and the collective contributions due to the phase phonons.[33] Sharp absorption bands are produced at the frequencies of each phase phonon for $\omega < 2\Delta$ (where 2Δ is the size of the gap), whereas for $\omega > 2\Delta$ sharp indentations occur at each phase phonon. The indentations exhibit an interference effect noted by Fano[17] in which the dip in the absorption spectrum is preceded by a peak on the low-frequency side. It is, therefore, possible to obtain an approximate value for the total gap, 2Δ, from the a_g-mode line shapes. From Fig. 3 we estimate that the gap is between 950 and 1200 cm^{-1} for $(NMP)_{0.55}(Phen)_{0.45}(TCNQ)$. This value is in reasonable agreement with numbers estimated from conductivity data.[7,21] Similar values of a gap are estimated for other x, although large error bars make quantitative comparison with the gaps obtained from conductivity difficult for these other compositions. For $Qn(TCNQ)_2$ we estimate the gap in the range 700–950 cm^{-1}. The change of shape of the infrared bands is most clearly observed by comparing ν_9 at 306 cm^{-1} with ν_5 at 1195 cm^{-1} and ν_4 at 1425 cm^{-1} in Fig. 2. The low-frequency mode is a peak raised above the background absorption, whereas for the higher-frequency modes there is a deep dip in the absorption with a peak at the low-frequency side. The above range of frequencies agrees with the gap found in $Qn(TCNQ)_2$ by fitting the temperature dependence of the conductivity:[8] $2\Delta = 1200$ K or 804 cm^{-1}. Note that these gap estimates in $Qn(TCNQ)_2$ and in the NMP-Phen system both correspond to the frequency of the change in the temperature dependence of the absorption coefficient.

Conwell and Howard[21] have suggested that the origin of the gap is primarily from a Peierls distortion, supplemented by a small additional potential V_0 having the same periodicity as the Peierls distortion. Though temperature-dependent $4k_F$ diffuse x-ray scattering has been reported,[4,5] no intermolecular distortion of the TCNQ chain has been observed in these materials, so that site inequivalence must give rise to the Perierls distortion[38] The existence of an additional potential on the TCNQ chain may arise from Coulomb effects or from the neighboring chains. In the first case, if the on-site Coulomb repulsion U is large, and the nearest-neighbor repulsion V_1 and the next-nearest-neighbor repulsion V_2 are related by $V_1 > 2V_2$, then the electrons on the chain will tend to occupy every other site.[35] In the latter case, for $(NMP)_x(Phen)_{1-x}(TCNQ)$ with $x=0.5$, the charged NMP's and neutral Phen's alternate along the chain, giving rise to a periodic potential (of periodicity $2a$) on the TCNQ chain. For x above 0.5, a Fourier component of the electrostatic potential with this periodicity will occur. The random arrangement of dipoles on the Qn chain in $Qn(TCNQ)_2$ will also result in a small Fourier component with the same periodicity. Whatever the cause, the amplitude of V_0 is expected to be small, although its effect on the T-dependent oscillator strengths is strong.[21]

If the gap were due just to a Peierls transition, then any extra electrons or holes, arising from doping effects, thermal effects, or accidently incorporated impurities, would be expected to give rise to kinks, or solitons, with levels at midgap.[11] However, in the presence of an additional potential, we expect bipolarons to be the stable configuration.

The temperature dependence of the oscillator strengths of eight of the a_g modes is shown in Fig. 7 for $Qn(TCNQ)_2$. For a pure Peierls transition, the modes should disappear abruptly at a critical temperature T_c. Instead, there is a slow decay of the a_g-mode intensity, indicating that the gap is present up to room temperature and beyond. This fact is also confirmed in temperature-dependent dc-conductivity measurements.[6,7] Figures 8 and 9 show the temperature dependence of the oscillator strengths of two of the a_g modes in the NMP-Phen system. The other a_g modes in this system were less temperature dependent and tended to be much more noisy.

The T dependence of the full gap is affected by the presence of an additional potential as well as by the production of solitons or polarons through doping and thermal effects. Conwell and Howard[21] have calculated the gap as a function of temperature for $Qn(TCNQ)_2$. They find that the gap equation decomposes into two terms, i.e., $\tilde{\Delta}_0(T) = \Delta_0(T) + \Delta_e$, where $\tilde{\Delta}_0(T)$ is half the full gap, $\Delta_0(T)$ is the Peierls-dependent portion, which also depends on the number of solitons and polarons present, and Δ_e is the external potential. Assuming 4% extra electrons in bipolaron states and allowing the number of thermally generated defect states to change with temperature, the full gap, calculated[21] for several values of the external potential, is shown in Fig. 7. The best fit

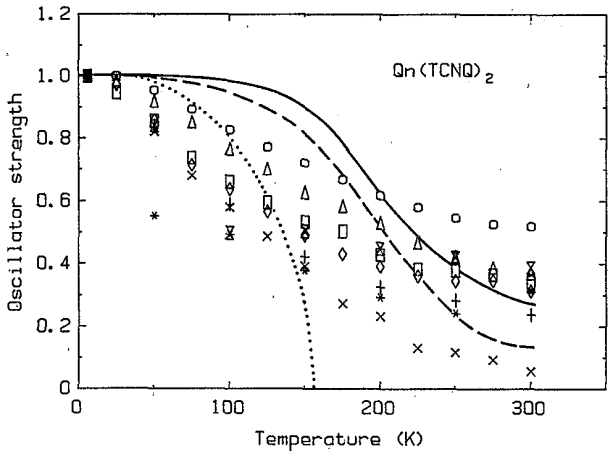

FIG. 7. Temperature dependence of the oscillator strength of eight a_g modes in $Qn(TCNQ)_2$: $\nu_3 = 1605$ cm^{-1} (□), $\nu_4 = 1425$ cm^{-1} (○), $\nu_5 = 1195$ cm^{-1} (△), $\nu_6 = 950$ cm^{-1} (×), $\nu_7 = 691$ cm^{-1} (◇), $\nu_8 = 600$ cm^{-1} (*), $\nu_9 = 306$ cm^{-1} (+), and $\nu_{10} = 124$ cm^{-1} (⧖). The curves shown represent the calculated gap for $Qn(TCNQ)_2$ from Ref. 21: the dotted line for $\Delta_e = 0$ K (i.e., no external potential), the dashed line for $\Delta_e = 10$ K, and the solid line for $\Delta_e = 25$ K.

to the measured oscillator strengths occurs (at least at the highest temperatures) for $\Delta_e = 25$ K.[21]

At lower temperatures (below 200 K) the data in Fig. 7 indicate a more rapid dropoff than the theoretical fit. Conwell and Howard[21] have suggested that because the samples exist in polycrystalline form, they will have a range of gaps above and below the average value. The presence of smaller gaps will result in a decrease of the a_g-mode intensities at lower temperatures than would occur for the average gap value.

For the $(NMP)_x(Phen)_{1-x}(TCNQ)$ samples, the T dependence of the oscillator strengths of the a_g modes has only weak variation with x (Figs. 8 and 9). This fact may reflect the role of the external potential Δ_e, in each of these compounds, reducing the T dependence of the a_g modes despite the variation from commensurate to incommensurate compositions.

It is well known that the presence of bipolarons introduces absorptions within the band gap.[39] The comparison of the optical-absorption data presented here to that of doped polyacetylene[40–42] and other polymers, such as polypyrrole,[43] polythiophene,[44,45] and polyaniline,[46,47] suggests that the in-gap absorption of $Qn(TCNQ)_2$ and $(NMP)_x(Phen)_{1-x}(TCNQ)$ may be due to electronic transitions to these bipolaron levels. While there is no sharp onset of absorption near the gap and no sharp absorptions within the gap that may be due to well-defined bipolaron levels, the very broad increase in absorption shown here is consistent with the interpretation of Conwell and Howard[21] of the existence of a range of gaps about some average gap value in these materials. Another possibility is that a range of energy levels for bipolaron states may exist. Conwell and Howard calculated[21] for an external potential of size $\Delta_e = 25$ K in $Qn(TCNQ)_2$ that the bipo-

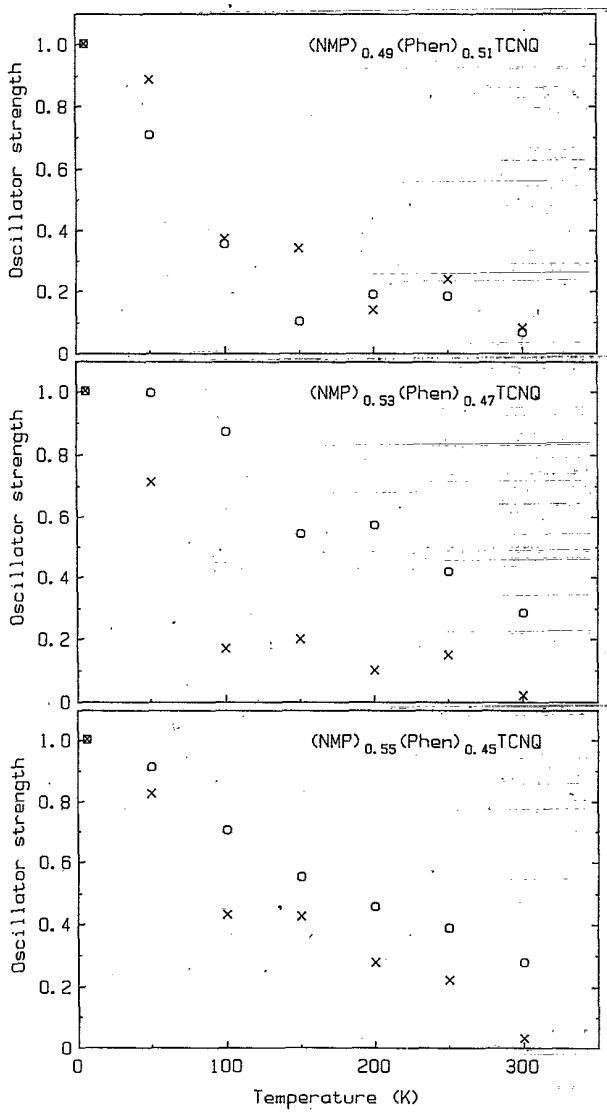

FIG. 8. Temperature dependence of the oscillator strength of $\nu_9 = 304$ cm^{-1} (×) and $\nu_{10} = 117$ cm^{-1} (○) in $(NMP)_x(Phen)_{1-x}(TCNQ)$ for $x = 0.49$ (top), 0.53 (middle), and 0.55 (bottom).

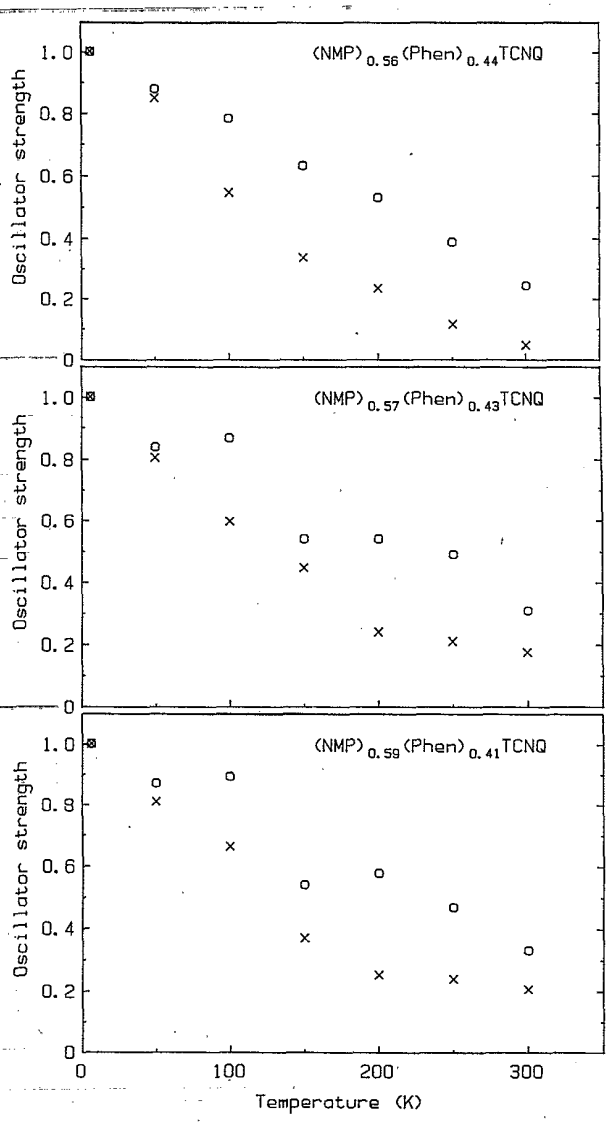

FIG. 9. Temperature dependence of the oscillator strength of $\nu_9 = 304$ cm^{-1} (×) and $\nu_{10} = 117$ cm^{-1} (○) in $(NMP)_x(Phen)_{1-x}(TCNQ)$ for $x = 0.56$ (top), 0.57 (middle), and 0.59 (bottom).

laron levels occur at $\omega_0=200$ K (140 cm^{-1}) above and below midgap. For $\Delta_e=10$ K, ω_0 was calculated as 125 K (90 cm^{-1}); for $\Delta_e=50$ K, $\omega_0=270$ K (190 cm^{-1}). Hence, we see that a range of values for the external potential gives rise to a range of values for the bipolarons levels.

In $(NMP)_x(Phen)_{1-x}(TCNQ)$, the magnitude of the absorption for frequencies below 2Δ does not scale as the number of bipolarons at low temperature, viz., $(x-0.5)/2$. However, for a given x the absorption does increase with increasing temperatures (Figs. 3 and 4), in accord with thermal generation of increasing numbers of bipolarons with increasing temperature.[11] The anomalous x-independent magnitude of the absorption below the gap may arise from the instantaneous creation and destruction of confined soliton-antisoliton pairs (bipolarons) via quantum nucleation[48] consistent with the Heisenberg uncertainty principle.

The sample-dependent spectra of Fig. 5 indicate several transitions to excited states. In the large-U case, the ground-state configuration of a Peierls distortion would imply a $2k_F$ or a $4k_F$ CDW, depending on the relative strengths of the transfer integral t, the nearest-neighbor Coulomb interaction V_1, and the next-nearest-neighbor Coulomb interaction V_2.[31,37] For small t, If $V_1>2V_2$, then electrons would be located on every other site resulting in a $4k_F$ dimer configuration $(0,-)$, where 0 represents a neutral site and $-$ represents an anion. If $V_1<2V_2$ the pairing of $[TCNQ]^-$ molecules would result in a $2k_F$ tetramer configuration $(0,-,-,0)$. As t becomes larger, the two configurations compete so that components of either configuration could be present depending on the relative values of V_1 and V_2.

The excitations at A, B, C, and D have commonly been interpreted,[31,49,50] respectively, as charge-transfer excitations CT1 (from $[TCNQ]^-$ to $[TCNQ]^0$) and CT2 (from $[TCNQ]^-$ to $[TCNQ]^-$), and as localized excitons (excitations of the TCNQ molecule), LE1 and LE2. A tetramer model calculation[31] shows that the CT2 transition falls in the vicinity of peak B. Yakushi *et al.*[49] have assigned peak B in other TCNQ salts to the exciton of the $[TCNQ]^-$ anion, $LE1^-$, consistent with a dimer model calculation and with $[TCNQ]^-$ solution spectra that show the characteristic splitting at peak B. This splitting is seen in many other TCNQ salts, as well as in the $x=0.53$ data of Fig. 5. The dimer model of Yakushi *et al.* also ascribes peak C in other salts to the triplet-state exciton of a $[TCNQ]^0$ and $[TCNQ]^-$ pair, and peak D to the singlet-state exciton of this same pair. However, the assignment of peak C to LE1 and peak D to LE2 for a pair of $[TCNQ]^-$'s is consistent with solution spectra for $[TCNQ]^-$ dimers.[50,51] It is noted that for samples of $x\gtrsim0.55$ peaks C and D become nearly unobservable. This change in the electronic spectra may reflect the crossover from an ordered commensurate electronic distribution ($x\lesssim0.55$), which can support localized intramolecular $[TCNQ]^-$ excitations, to an incommensurate distribution ($x\gtrsim0.57$), which can no longer support these excitations. A more thorough theoretical examination of these materials is needed to clarify the variation of these competing interactions with x and the effects upon the electronic spectra in Fig. 5. These calculations, within the context of a tetramer model, so as to incorporate on-site and long-range Coulomb interactions, should include lower-lying energy levels and their associated electrons in order to understand the transitions and energies involved.

V. SUMMARY

In summary, we have measured the optical properties of $Qn(TCNQ)_2$ and $(NMP)_x(Phen)_{1-x}(TCNQ)$ for $0.5\lesssim x\lesssim0.6$. Several important interactions involving the unpaired electrons on the TCNQ chains have been examined, including excitation energies, charge-transfer interactions, the Peierls distortion, and electron-phonon interactions. The existence of a gap in these materials has been established (up to room temperature) and has been shown to be due predominantly to a Peierls distortion. A small contribution to the potential of the TCNQ chains, with the same periodicity as the Peierls distortion, causes a slow decay in the size of the gap as temperature increases. This external potential may be the cause of almost no change in the spectra with variation of x. The low-energy spectra (below 2Δ) may be absorption due to quantum-nucleated solitons or bipolarons, as well as thermally activated solitons and bipolarons at higher temperatures. The electronic structure at higher energies is indicative of charge-transfer and excitonic interactions and reflects the crossover from a commensurate distribution of electronic charge for $x\lesssim0.57$ to an incommensurate distribution for $x\gtrsim0.57$.

ACKNOWLEDGMENTS

This research was supported in part by National Science Foundation–Solid State Chemistry Grant No. DMR-84-16511 and by the Defense Advanced Research Projects Agency through a grant monitored by the U.S. Office of Naval Research.

*Present address: RIFA AB, S-11100 Stockholm, Sweden.

[1]H. Kobayashi, F. Marumo, and Y. Saito, Acta. Crystallogr. Sect. B **27**, 373 (1971).

[2]J. S. Miller and A. J. Epstein, J. Am. Chem. Soc. **100**, 1639 (1978).

[3]C. J. Fritchie, Acta. Crystallogr. **20**, 892 (1966).

[4]J. P. Pouget, S. Megtert, R. Comes, and A. J. Epstein, Phys. Rev. B **21**, 486 (1980).

[5]A. J. Epstein, J. S. Miller, J. P. Pouget, and R. Comes, Phys. Rev. Lett. **47**, 741 (1981).

[6]A. A. Gogolin, S. P. Zolotukhin, V. I. Mel'nikov, E. I. Rashba, and I. F. Shchegolev, Pis'ma Zh. Eksp. Teor. Fiz. **22**, 564 (1975) [JETP Lett. **22**, 278 (1975)].

[7]A. J. Epstein, J. W. Kaufer, H. Rommelmann, I. A. Howard, E. M. Conwell, J. S. Miller, J. P. Pouget, and R. Comes, Phys. Rev. Lett. **49**, 1037 (1982).

[8]A. J. Epstein and E. M. Conwell, Solid State Commmun. **24**, 627 (1977); A. J. Epstein and J. S. Miller, *ibid.* **27**, 325 (1978);

A. J. Epstein, E. M. Conwell, and J. S. Miller, Ann. N.Y. Acad. Sci. **313**, 183 (1978).
[9]A. N. Bloch, R. B. Weisman, and C. M. Varma, Phys. Rev. Lett. **28**, 753 (1972).
[10]S. Alexander, J. Bernasconi, W. R. Schneider, R. Biller, W. G. Clark, G. Gruner, R. Ohrbach, and A. Zettl, Phys. Rev. B **24**, 7474 (1981).
[11]M. J. Rice and E. J. Mele, Phys. Rev. B **25**, 1339 (1982); I. A. Howard and E. M. Conwell, *ibid.* **27**, 6205 (1983); H. H. S. Javadi, Joel S. Miller, and A. J. Epstein, Phys. Rev. Lett. **59**, 1760 (1987).
[12]J. F. Kwak, G. Beni, and P. M. Chaikin, Phys. Rev. B **13**, 641 (1976); P. M. Chaikin, J. F. Kwak, and A. J. Epstein, Phys. Rev. Lett. **42**, 1178 (1979).
[13]A. J. Epstein, J. S. Miller, and P. M. Chaikin, Phys. Rev. Lett. **43**, 1178 (1979).
[14]L. M. Bulaevskii *et al.*, Zh. Eksp. Teor. Fiz. **62**, 725 (1972) [Sov. Phys.—JETP **5**, 384 (1972)].
[15]R. E. Peierls, *Quantum Theory of Solids* (Oxford University Press, London, 1955), p. 108.
[16]M. J. Rice, Phys. Rev. Lett. **37**, 36 (1976).
[17]U. Fano, Phys. Rev. **124**, 1866 (1961).
[18]E. F. Steigmeier, H. Auderset, D. Baeriswyl, M. Almeida, and K. Carneiro, J. Phys. (Paris) Colloq. **44**, C3-1445 (1983); J. E. Eldridge, N. Fortier, F. E. Bates, and J. S. Miller, *ibid.* **44**, C3-1465 (1983).
[19]S. Etemad, Phys. Rev. B **24**, 4959 (1981).
[20]R. Bozio, C. Pecile, and P. Tosi, J. Phys. (Paris) Colloq. **44**, C3-1453 (1983).
[21]E. M. Conwell and I. A. Howard, Phys. Rev. B **31**, 7835 (1985); J. Phys. (Paris) Colloq. **44**, C3-1487 (1983); Synth. Met. **13**, 71 (1986).
[22]K. D. Cummings, D. B. Tanner, and J. S. Miller, Phys. Rev. B **24**, 4142 (1981).
[23]R. B. Sanderson and H. E. Scott, Appl. Opt. **10**, 1097 (1971).
[24]J. C. Maxwell Garnett, Philos. Trans. R. Soc. London **203**, 385 (1904); **205**, 237 (1906).
[25]Y. H. Kim (private communication).
[26]G. L. Carr, Ph.D. thesis, The Ohio State University, 1982.
[27]F. Paschen, Ann. Phys. (Leipzig) **26**, 136 (1908).
[28]R. P. McCall, D. B. Tanner, J. S. Miller, A. J. Epstein, I. A. Howard, and E. M. Conwell, Synth. Met. **11**, 231 (1985).
[29]R. P. McCall, D. B. Tanner, J. S. Miller, A. J. Epstein, I. A. Howard, and E. M. Conwell, Mol. Cryst. Liq. Cryst. **120**, 59 (1985).
[30]A. J. Epstein, R. W. Bigelow, J. S. Miller, R. P. McCall, D. B. Tanner, Mol. Cryst. Liq. Cryst. **120**, 43 (1985).
[31]D. B. Tanner, I. Hamberg, C. S. Jacobsen, M. Almeida, K. Carneiro, A. J. Epstein, and J. S. Miller, Physica B+C **143B**, 471 (1986).
[32]R. Bozio, I. Zanon, A. Girlando, and C. Pecile, J. Chem. Soc. Faraday Trans. I **74**, 235 (1978).
[33]M. J. Rice, L. Petronero, P. Bruesch, Solid State Commun. **21**, 757 (1977).
[34]M. J. Rice, V. M. Yartsev, and C. S. Jacobsen, Phys. Rev. B **21**, 3437 (1980).
[35]R. P. McCall, D. B. Tanner, J. S. Miller, and A. J. Epstein, Phys. Rev. B **35**, 9209 (1987).
[36]S. Mazumdar, S. N. Dixit, and A. N. Bloch, Phys. Rev. B **30**, 4842 (1984).
[37]J. Hubbard, Phys. Rev. B **17**, 494 (1978).
[38]E. M. Conwell, A. J. Epstein, and M. J. Rice, in *Quasi-One-Dimensional Conductors I*, edited by S. Barišić, A. Bjeliš, J. R. Cooper, and B. Leontić (Springer-Verlag, Berlin, 1979), p. 204.
[39]K. Fesser, A. R. Bishop, and D. K. Campbell, Phys. Rev. B **27**, 4804 (1983).
[40]N. Suzuki, M. Ozaki, S. Etemad, A. J. Heeger, and A. G. MacDiarmid, Phys. Rev. Lett. **45**, 1209 (1980).
[41]A. J. Epstein, H. Rommelmann, R. Bigelow, H. W. Gibson, D. M. Hoffman, and D. B. Tanner, Phys. Rev. Lett. **50**, 1866 (1983).
[42]X. Q. Yang, D. B. Tanner, A. Feldblum, H. W. Gibson, M. J. Rice, and A. J. Epstein, Mol. Cryst. Liq. Cryst. **117**, 267 (1985).
[43]J. L. Bredas, J. C. Scott, K. Yakushi, and G. B. Street, Phys. Rev. B **30**, 1023 (1984).
[44]T.-C. Chung, J. H. Kaufman, A. J. Heeger, and F. Wudl, Phys. Rev. B **30**, 702 (1984).
[45]D. Bertho and C. Jouanin, Phys. Rev. B **35**, 626 (1987).
[46]A. J. Epstein, J. M. Ginder, F. Zuo, R. W. Bigelow, H. S. Woo, D. B. Tanner, A. F. Richter, W. S. Huang, and A. G. MacDiarmid, Synth. Met. **18**, 303 (1987).
[47]S. Stafström, J. L. Brédas, A. J. Epstein, H. S. Woo, D. B. Taner, W. S. Huang, A. G. MacDiarmid, Phys. Rev. Lett. **59**, 1464 (1987).
[48]J. P. Sethna and S. Kivelson, Phys. Rev. B **26**, 3513 (1982); S. Kivelson and J. P. Sethna, J. Phys. (Paris) Colloq. **44**, C3-657 (1983); A. Auerbach and S. Kivelson, Phys. Rev. B **33**, 8171 (1986).
[49]K. Yakushi, M. Iguchi, G. Katagiri, T. Kusaka, T. Ohïta, and H. Kuroda, Bull. Chem. Soc. Jpn. **54**, 348 (1981).
[50]Y. Iida, Bull. Chem. Soc. Jpn. **42**, 637 (1969).
[51]R. H. Boyd and W. D. Phillips, J. Chem. Phys. **43**, 2927 (1965).